OPEN

# Longitudinal trajectories of brain volume in combined antiretroviral therapy treated and untreated simian immunodeficiency virus-infected rhesus macaques

Dan Liu[a,*], Jiaojiao Liu[a,*], Tingting Xu[g], Hongwei Qiao[h], Yu Qi[a], Yuxun Gao[a], Ailixire[b], Lei Gao[i], Chunlin Li[c], Mingrui Xia[d,e,f] and Hongjun Li[a,b]

**Objectives:** We used simian immunodeficiency virus (SIV)-infected nonhuman primates to investigate longitudinal changes of brain volume caused by SIV and the effect of combined antiretroviral therapy (cART). In addition, the relation between viral load, immune status, and brain volume were explored.

**Design:** A longitudinal study of two healthy controls, five $SIV_{mac239}$-infected macaques received cART (SIV+cART+) at 40 days postinnoculation, and five $SIV_{mac239}$-infected macaques received no therapy (SIV+cART−).

**Methods:** Structural T1-weighted MRI, blood and cerebrospinal fluid testing were acquired at multiple time points for 48 weeks postinfection (wpi). Brain volume was estimated using region of interest (ROI)-based analysis. Volume differences were compared among three groups. Linear regression models tested the associations between brain volumes and biomarkers (viral load, $CD4^+$ T-cell count, $CD4^+/CD8^+$ ratio).

**Results:** In our model, brain volume alteration in SIV-infected macaques can be detected at 12 wpi in several brain regions. As the infection progresses, the SIV+cART− − macaques displayed generalized gray matter atrophy at the endpoint. Though initiate cART right after acute infection, SIV+cART+ macaques still displayed brain atrophy but showed signs of reversibility. Plasma viral load is mainly associated with subcortical nucleus volume whereas $CD4^+$ T-cell count and $CD4^+/CD8^+$ ratio in plasma were associated with widespread cortical volume.

**Conclusion:** The $SIV_{mac239}$-infected Chinese origin macaque is a valid model for neuroHIV. Brain atrophy caused by SIV infection can be relieved, even reversed, by cART. Our model also provides new insights into understanding the pathogenesis of brain injury in people with HIV (PWH).



*AIDS* 2021, **35**:2433–2443

**Keywords: combined antiretroviral therapy, macaque, simian immunodeficiency virus, structural MRI**

[a]Department of Radiology, Beijing Youan Hospital, Capital Medical University, [b]Beijing Advanced Innovation Centre for Biomedical Engineering, Beihang University, [c]School of Biomedical Engineering, Capital Medical University, [d]State Key Laboratory of Cognitive Neuroscience and Learning, [e]Beijing Key Laboratory of Brain Imaging and Connectomics, [f]IDG/McGovern Institute for Brain Research, Beijing Normal University, Beijing, China, [g]Division of Neurogeriatrics, Department of Neurobiology, Care Sciences and Society, Karolinska Institutet, Stockholm, Sweden, [h]Institute of Laboratory Animal Sciences, Chinese Academy of Medical Sciences, Beijing, and [i]Department of Radiology, Zhongnan Hospital of Wuhan University, Wuhan, China.

Correspondence to Hongjun Li, MD, Beijing Youan Hospital, Capital Medical University, No. 8, Xi Tou Tiao, Youanmen Wai, Fengtai District, Beijing 100069, China.

E-mail: lihongjun00113@ccmu.edu.cn

[*] Dan Liu and Jiaojiao Liu contributed equally to this work.

Received: 8 January 2021; revised: 7 August 2021; accepted: 10 August 2021.

DOI:10.1097/QAD.0000000000003055

## Introduction

HIV penetrates the central nervous system (CNS) soon after infection, activating resident glial cells and triggering infiltration of periphery monocytes/macrophages as well. These cells release viral proteins and produce inflammatory factors, resulting in prominent inflammation, immune activation and suppression, and blood–brain barrier disruption, all of which contribute to neuronal injury, even apoptosis [1]. Combined antiretroviral therapy (cART) suppresses viral replication systemically, and partially restores immune functions but cannot eliminate viral proteins in the brain [2], which were associated with oligodendroglial population reduction, dendritic spins loss, and synaptic protein disruption shown in transgenic animal models [3–5]. In addition, the iatrogenic effects of drugs on brain integrity are also of concern [6,7]. The neuropathogenesis of HIV-associated brain damage remains to be elucidated. Brain volume analysis conducted by MRI is helpful to detect brain morphologic alteration, which was hypothesized to be related to neurogenesis, myelination density, number or size of neuron or glia, angiogenesis, dendritic spine size, and density [8–11], and has the potential to shed light on the pathogenesis of HIV-induced brain damage.

Previous studies reported subcortical nucleus, white matter, and cortical atrophy in people with HIV (PWH) [12–14], whereas there are also researches failed to find any alterations [15], some even reported increased brain volume in PWH [16,17]. However, most clinical studies were cross-sectional with lots of confounders (such as age, ethnicity, living environment, duration of infection, complications, different treatment regimens), which are difficult to determine or control [14,18,19]. For the limited longitudinal studies, the durations of studies are always short relative to the course of this condition with few time points and lack of premorbid condition of the brain [20–23]. Reliable animal model and solid experiment design are needed to settle these issues.

Studies show nonhuman primates infected with simian immunodeficiency virus (SIV) resulting in $CD4^+$ T-cell depletion and development of systematic immunodeficiency, exhibiting pathogenesis and pathological processes similar to those seen in HIV-infected patients [24] and have been widely employed to explore the neuropathogenesis, therapy strategies [25,26]. Among the various models, the Chinese-origin rhesus macaque infected with $SIV_{mac239}$ demonstrates close pathogenesis to HIV-1-infected humans [27], and might serve as a qualified model of neuroHIV.

In this longitudinal study, we aimed to map the natural course of brain structural changes during SIV infection and the impact of cART and explore the relationship between brain volume changes and blood, cerebrospinal fluid (CSF) biomarkers.

## Methods

### Rhesus macaques, simian immunodeficiency virus, and treatment regime

Twelve healthy male Chinese-origin rhesus macaques (weight: $4.7 \pm 0.6$ kg; age: $3.8 \pm 0.3$ years) were used in our study. All macaques were screened and seronegative for tuberculosis, Salmonella, Shigella, Ecto Parasite, Endo Parasite, simian-T-lymphotropic virus-1, simian type D retrovirus, herpes B virus, as well as SIV antibody before incubation. During the experiment, our macaques were quarantined every 6 months, and all macaques were negative for human *Mycobacterium tuberculosis* and *Mycobacterium bovis*.

Ten macaques were intravenously inoculated with a 50-fold half tissue culture infective dose ($TCID_{50}$) of $SIV_{mac239}$ through the brachial vein and were all seroconverted to SIV within 7 days after inoculation. Five of them received cART 40 days after inoculation (SIV+cART+), whereas the other five macaques received no treatment (SIV+cART−). The treatment regime included Emtricitabine (50 mg/kg per day), Tenofovir disoproxil fumarate (5.1 mg/kg per day), and Dolutegravir (2.5 ml/kg per day) (see Supplementary Material for details, http://links.lww.com/QAD/C267).

### Ethics statement

The study was approved by the Institutional Animal Care and Use Committee (IACUC) at the Institute of Laboratory Animal Science, Chinese Academy of Medical Sciences (IACUC Approval No: LHJ18001), and performed according to the recommendations in the Guide for the Care and Use of Laboratory Animals of the Institute of Laboratory Animal Science and the recommendations of the Weatherall report for the use of nonhuman primates in research (http://www.acmedsci.ac.uk/more/news/the-use-of-nonhuman-primates-in-research/) to ensure personal safety and animal welfare. All macaques were housed and fed in an Association for Assessment and Accreditation of Laboratory Animal Care (AAALAC)-accredited bio-safety level 3 laboratory.

A detailed description of the living environment and housing facilities can be found in previous research [28].

### Anesthesia and euthanasia

All experimental procedures (physical examination, imaging acquisition, blood extraction, lumbar puncture) were performed under anesthesia. Each macaque was intramuscularly injected with atropine (0.05 mg/kg) to decrease bronchial and salivary secretions and Zoletil 50 (5 mg/kg) to achieve an anesthetic effect. The anesthesia depth was assessed by monitoring corneal reflex, toe-pinch reflex, heart rate, and respiration rate. With this dosage, the anesthesia could be maintained for about 1 h.

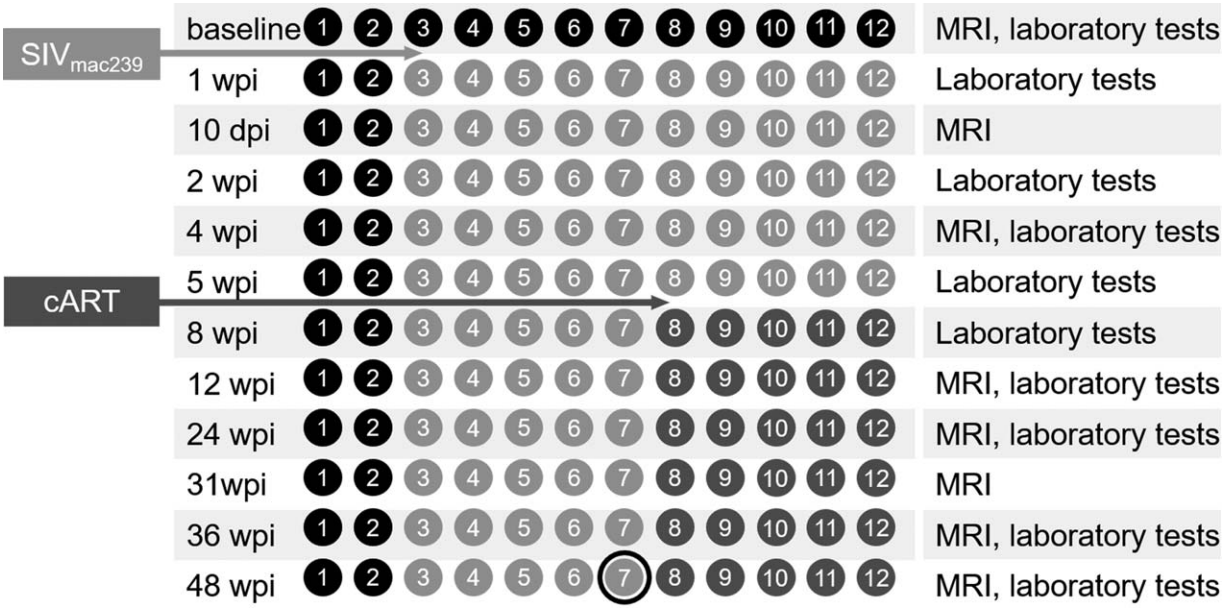


**Fig. 1. Study design.** A total of 12 macaques were involved in our study. MRI and laboratory tests were collected at baseline and subsequent time points. Ten macaques (light gray) were intravenously inoculated with $SIV_{mac239}$. Five received cART 40 days after inoculation (dark gray), whereas the other five macaques received no treatment (light gray). A black circle marked the endpoint in SIV+cART− group. Macaque 7 was euthanized at 47 wpi. SIV, simian immunodeficiency virus.

The decision to euthanize was based on clinical signs of simian-acquired immunodeficiency syndrome (AIDS), including weight loss of more than 10%, chronic anorexia, chronic diarrhea, mental state. One macaque (macaque 7) was euthanized at 47 wpi, data collected before euthanasia was included in 48 wpi for analysis. The study design was shown in Fig. 1.

## Laboratory tests

Laboratory data were acquired at baseline (before inoculation), a week postinfection, 2, 5, 8, 12, 24, 36, and 48 wpi. These time points were set in consideration of the virus reported to be detectable in the CNS a week after infection [29] and physiological condition. Viral load in plasma and CSF were detected by measuring SIV RNA levels (extracted by TRIzol) by reverse transcription-PCR (RT-PCR) as previously described. $CD4^+$ T-cell and $CD8^+$ T-cell counts in the peripheral blood were analyzed by flow cytometry (see Supplementary Material for details, http://links.lww.com/QAD/C267).

## Data acquisition

MRI examination was performed at baseline (before infection), 10 days postinfection (dpi), 4, 12, 24, 31, 36, and 48 wpi. All data were acquired via a Siemens Trio Tim 3T-scanner with a 32-channel head coil. Fluid-attenuated inversion recovery imaging was performed to rule out the presence of brain lesions. Structural images were collected using a T1-weighted magnetization prepared gradient-echo sequence (72 axial slices, about 6 min; repetition time, 1800 ms; echo time, 4.12 ms; resolution matrix, $192 \times 192$; flip angle, 9°; slice thickness, 1 mm; voxel size, 1 mm × 1mm × 1 mm).

## Image processing

Skull and other tissue outside of the brain were manually removed to obtain more accurate brain extraction. Subsequent procedures were carried out by SPM12 (Statistical Parametric Mapping 12, https://www.fil.ion.ucl.ac.uk/spm/). First, T1-weighted images were augmented 2.6 times to make the monkey's brain size comparable with that of human's, thus more appropriate to analyze using SPM [30]. Second, all skull-striped T1 images were denoised by Spatially Adaptive Non-Local Means (SANLM) in computational anatomy toolbox 12 (CAT12, http://www.neuro.uni-jena.de/cat/). Third, the denoised T1 images were segmented and normalized to the INIA19 tissue probability maps [31] employing affine transformation. Fourth, all affine transformed images were used to create a customized template. Finally, all gray matter, white matter, CSF files in native space generated previously were normalized to Montreal Neurological Institute (MNI) space and smoothed with an isotropic Gaussian kernel of full width at half maximum of 4 mm.

Volumes were extracted from 21 ROIs, including total gray matter volume (GMV), white matter volume (WMV), lateral ventricles, caudate, putamen, hippocampus, frontal lobe, occipital lobe, parietal lobe, temporal lobe, insula, and cerebellum, representative of the whole brain. We also made an extra 81 ROIs according to the INIA19 atlas to figure out whether we can get the same

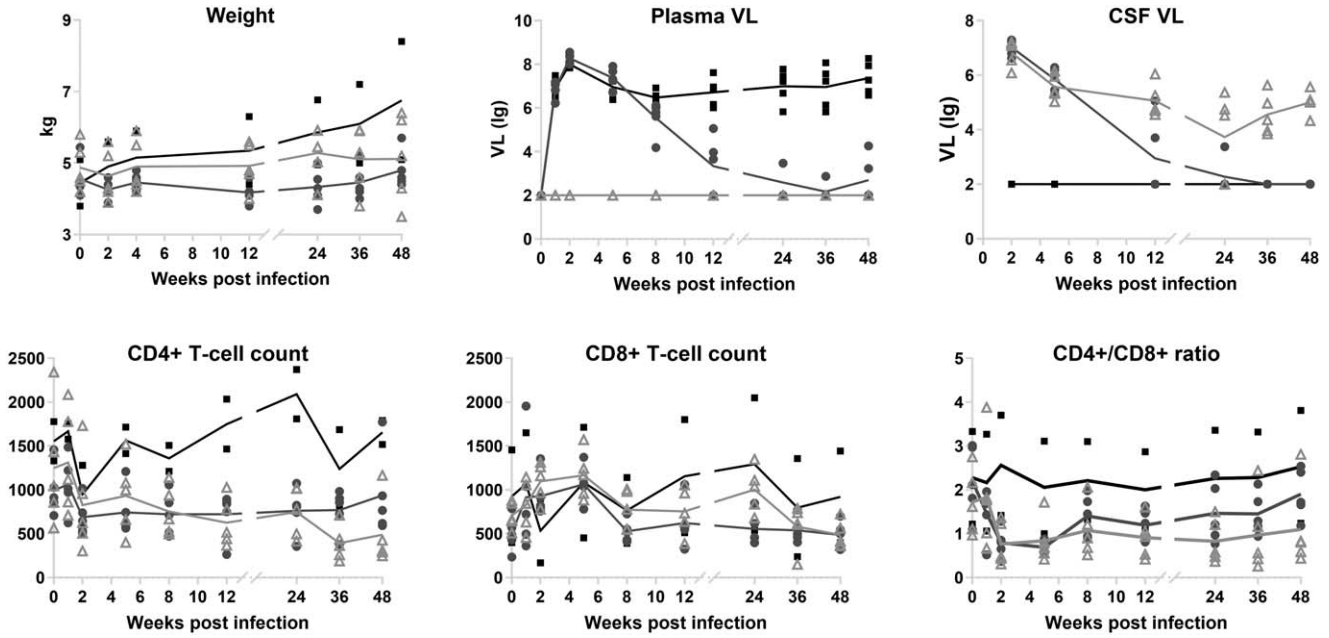


**Fig. 2. Weight, viral load, peripheral blood CD4$^+$ T-cell count, CD8$^+$ T-cell count, and CD4$^+$/CD8$^+$ ratio trajectories of rhesus macaques in three groups.** Black: healthy control group; light gray: SIV-infected without therapy; dark gray: SIV-infected with therapy.

results for smaller ROIs (Supplementary Material, http://links.lww.com/QAD/C267).

The relative volume (volume%) of each ROI was calculated. The volume% of each ROI was calculated by dividing the volume at each time point by the volume at baseline ($V_{time}/V_{baseline}$). By applying relative ROI volumes, we were able to eliminate intracranial volume differences among macaques and volume differences in ROIs.

### Statistical analysis

Age and weight at baseline were compared among three groups using nonparametric Kolmogorov–Smirnov one-way analysis of variance (ANOVA). Viral load was log-transformed. Weight, viral load, immunological markers, and volume% of ROIs were compared using the generalized estimating equations (GEE) model to test whether the trajectories differed among groups. Volume% differences between healthy macaques and SIV+cART− group at 10 dpi and 4 wpi were compared using the Mann–Whitney *U*-test. All the above analyses were performed using IBM Statistics version 22 (IBM, Armonk, New York, USA). A *P* value less than 0.05 was considered statistically significant.

The relationship between GMV and laboratory results was tested by the linear regression model. All the analyses were corrected for multiple comparisons (GRF correction, voxel-level $P < 0.001$, cluster level $P < 0.05$, two-tailed).

## Results

### Viral load, CD4$^+$ T-cell count, and CD4$^+$/CD8$^+$ ratio trajectories in three groups

Differences in age and weight at baseline were not significant (age, $P = 0.594$; weight, $P = 0.509$). Longitudinal changes in weight, viral load, immunological markers are illustrated in Fig. 2. A significant time by group interaction was detected in weight ($P < 0.001$), plasma viral load ($P < 0.001$), CSF viral load ($P < 0.001$), peripheral blood CD4$^+$ T-cell count ($P < 0.001$), CD4$^+$/CD8$^+$ ratio ($P < 0.001$), which supported increasingly divergent trajectories among three groups.

Weight in the healthy control group showed a sustained increase whereas SIV+cART− group showed weight loss after 24 wpi, SIV+cART+ group showed a slight weight increase starting at 12 wpi.

A dramatic increase in plasma viral load was observed, and viremia reached its peak within 2 weeks in all SIV-infected macaques. Viral load declined subsequently and reached a plateau in 8 weeks. Macaques received cART showed continuous viral load decline. Viral load in CSF decreased to a nadir at 24 wpi and rose again afterward in SIV+cART− group; with cART, viral load in CSF dropped more sharply and was undetectable in three macaques at 12 wpi.

CD4$^+$ T-cell count, CD8$^+$ T-cell count, and CD4$^+$/CD8$^+$ ratio fluctuated even in healthy macaques but the overall trends were stable. SIV infection resulted in

significant $CD4^+$ T-cell count and $CD4^+/CD8^+$ ratio reduction, which can be stopped by cART. $CD4^+/CD8^+$ ratio showed an increasing tendency with the introduction of cART.

## Region of interest-based brain volume changes over time

Significant time by group interactions on volume% were detected in all 21 ROIs (all $P < 0.001$), suggesting volume% trajectories of all ROIs differed among groups. In general, SIV-infected macaque showed smaller gray matter than healthy controls, and GMV reduced more rapidly, with SIV+cART− group showed steeper negatively sloped trend lines than the healthy control group and SIV+cART+ group (Fig. 3). Further comparisons between groups at different time points showed that brain volume differences between healthy controls and SIV-infected macaques can be detected as early as 12 wpi, including differences in total gray matter, total white matter volume, lateral ventricle volume, right caudate, left putamen, bilateral hippocampus, bilateral frontal lobe, bilateral temporal lobe, left insular, and right cerebellum. As the infection continuous and the course progresses, at 48 wpi, the SIV+cART− macaques displayed smaller gray matter volume in caudate, putamen, hippocampus, frontal lobe, parietal lobe, temporal lobe, insula, and cerebellum compared with healthy controls. However, for macaques that received cART, only left hippocampus, right caudate, left parietal, bilateral temporal showed gray matter volume differences compared with healthy controls (Fig. 4).

Heat maps of 81 ROIs at 10 dpi, 4, 12, 24, 36, and 48 wpi of each macaque showed that macaque 3 and macaque 7 showed the most obvious atrophy at 48 wpi, especially for macaque 7 (macaque 7 was euthanized at 47 wpi, macaque 3 was euthanized later at 58 wpi). Both macaques showed widespread atrophy including all the studied cortical cortex, subcortical nucleus, limbic system. White matter atrophy was relatively mild. Interestingly, in the SIV+cART+ group, one macaque showed widespread brain atrophy soon after infection, continued to 36 wpi though this macaque showed undetected viral load. However, an overall increase in gray matter volume was detected at 48 wpi (Supplementary Figure 1, http://links.lww.com/QAD/C266). Interestingly, this macaque showed a sharp reduction in plasma $CD4^+$ T cell after infection and showed continuous low levels until 48 wpi. Total GMV showed significant association with $CD4^+$ T cell ($R = 0.914$, $P = 0.030$), suggesting poor immune reconstruction may aggravate brain atrophy.

Bilateral lateral ventricle volume in the healthy control group and SIV+cART− group increased over time. However, lateral ventricle no longer increased with time when controlled for the weight ($P > 0.050$), suggesting lateral ventricle increase in the healthy control group may be because of brain growth and development. In SIV+cART− group, lateral ventricle increased with time, even controlled for weight ($r = 0.505$, $P = 0.012$). Brain atrophy is likely to contribute to the expansion of lateral ventricle in SIV+cART− macaques.

## Gray matter volume correlates with viral load and systemic immune status

In SIV+cART− group, viral load in plasma was mainly associated with the volume of clusters in the subcortical nucleus, including bilateral putamen, bilateral caudate, left claustrum, and right hippocampus. In addition, the volume of few clusters in the cortical cortex (including left inferior/superior temporal gyrus, cerebellum lobe V, anterior quadrangular, simple lobe, left supramarginal gyrus, and left angular gyrus) were also associated with viral load in plasma (Fig. 5). The volume of clusters in the cortical cortex (including right middle/inferior frontal gyrus, bilateral PCC (extend to precuneus, postcentral gyrus), left supramarginal gyrus (extend to superior temporal gyrus, superior parietal lobule)) and subcortical nucleus (right thalamus) positively correlated with $CD4^+$ T-cell count (Supplementary Fig. 2, http://links.lww.com/QAD/C266). The volume of clusters in the cortical cortex [including bilateral superior/inferior semilunar lobule (extend to left fusiform, left simple lobule), inferior cerebellar peduncle, bilateral superior/middle temporal gyrus, bilateral anterior cingulate cortex, right lateral orbital gyrus, bilateral inferior/middle frontal gyrus, bilateral posterior cingulate cortex, left supramarginal gyrus] and subcortical nucleus [bilateral thalamus (extend to the superior colliculus, parasubicular area), right putamen (extend to right lateral globus pallidus)] positively correlated with $CD4^+/CD8^+$ ratio whereas the volume of clusters in left inferior temporal gyrus, right occipital lobe showed a negative correlation (Supplementary Fig. 3, http://links.lww.com/QAD/C266).

In the SIV+cART+ group, the brain regions correlated with plasma and CSF biomarkers were different from those detected in SIV+cART− group. The volume of clusters in the cortical cortex (including bilateral middle/superior temporal gyrus, bilateral insula, bilateral supramarginal gyrus, bilateral superior parietal lobule, bilateral angular gyrus, bilateral precentral gyrus, left postcentral gyrus, bilateral precuneus, left middle frontal gyrus, bilateral superior frontal gyrus, bilateral straight gyrus, bilateral anterior cingulate cortex, right frontoorbital gyrus, anterior quadrangular lobule, and lobule V/IV of the cerebellum) and subcortical nucleus (including bilateral putamen, bilateral caudate, left lateral globus pallidus, right claustrum) positively correlated with viral load in plasma (Supplementary Fig. 4, http://links.lww.com/QAD/C266). Multiple clusters in the cortical cortex, including bilateral frontal (precentral gyrus, orbital gyrus, straight gyrus, ACC, superior/middle/inferior frontal gyrus), temporal (superior/middle/

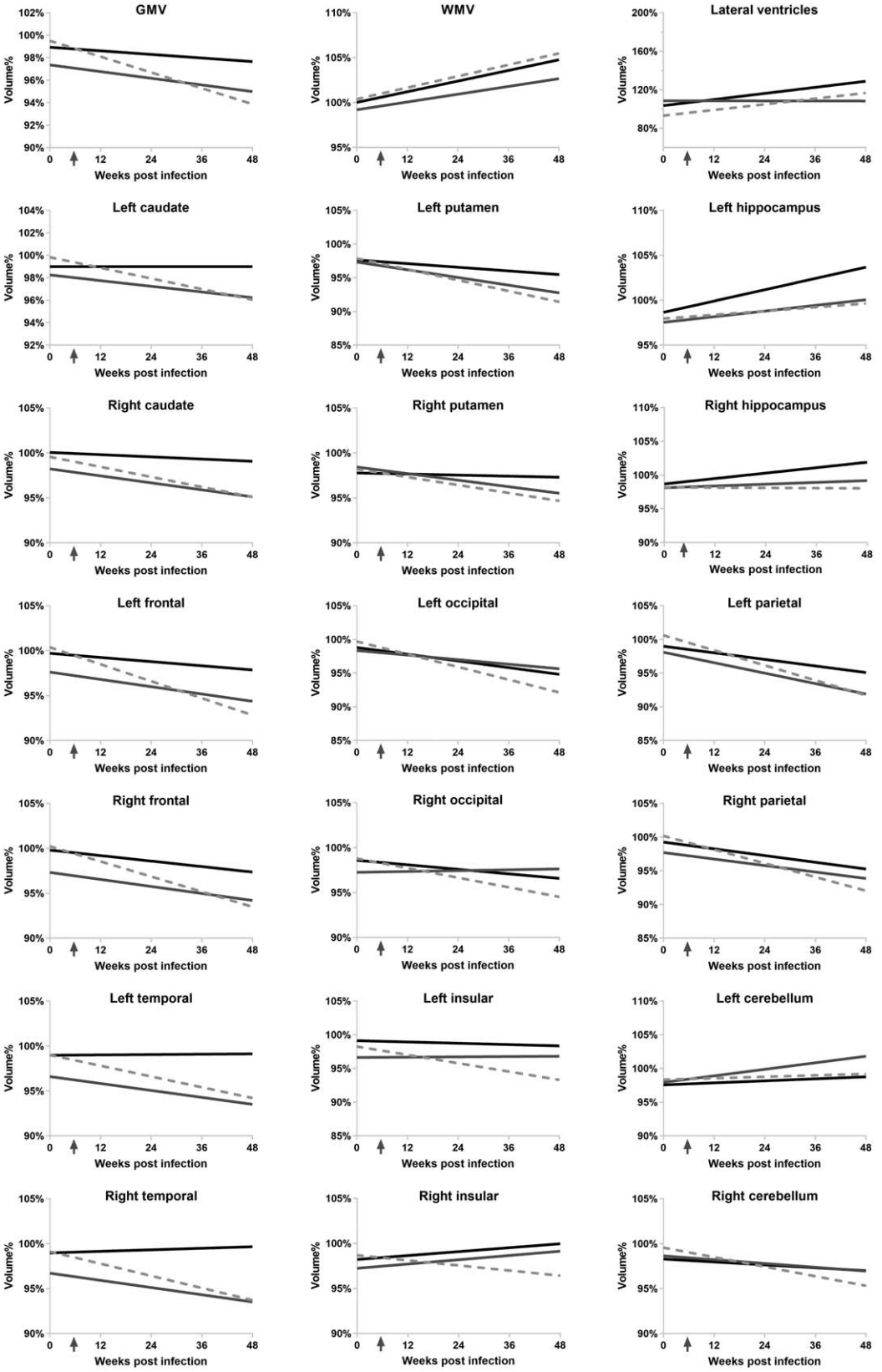


**Fig. 3. Volume percentage (volume%) trend lines of each region of interest in three groups.** Black line: healthy control group; light gray dashed line: SIV-infected without therapy; dark gray line: SIV-infected with therapy. SIV, simian immunodeficiency virus.

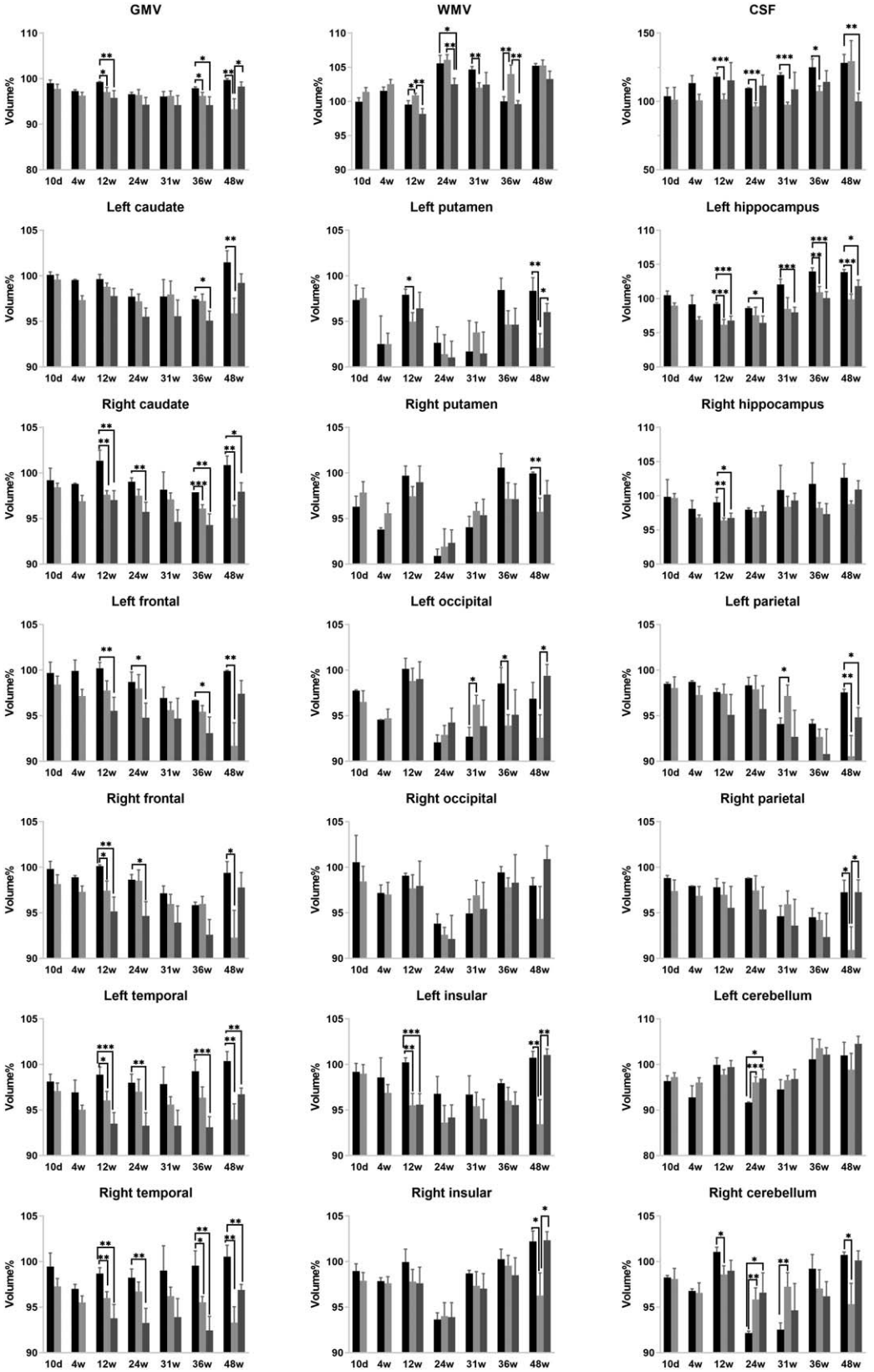


**Fig. 4. Volume percentage (volume%) of each region of interest at different time points in three groups.** Comparisons between groups were shown. Bars, mean ± SE. **P* less than 0.05; ***P* less than 0.01; ****P* less than 0.001. Black, healthy control; light gray, SIV-infected macaque without treatment; dark gray, SIV-infected macaque with treatment.

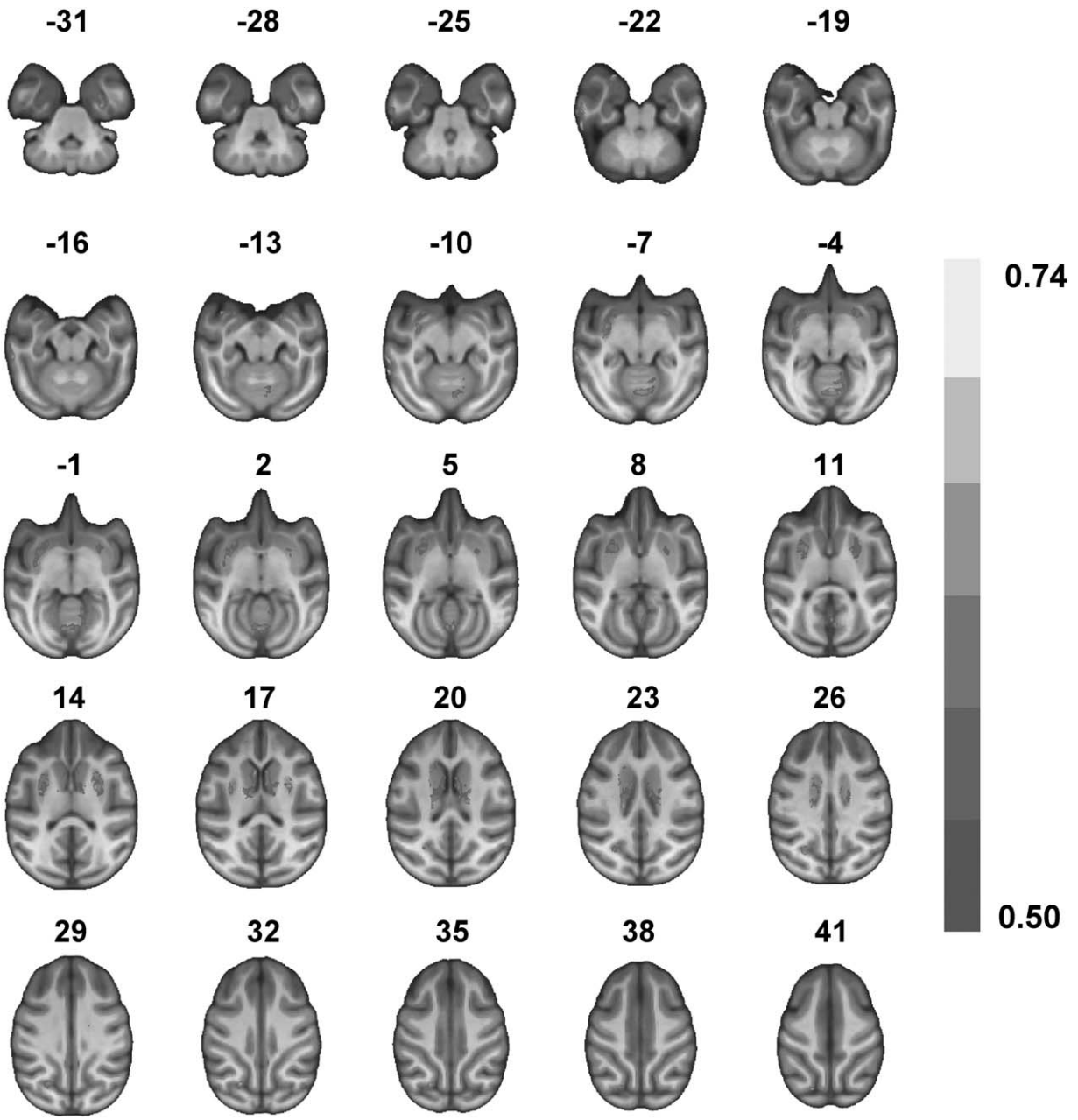


**Fig. 5. Gray matter volume of clusters associated with plasma viral load in SIV+cART− group.** Clusters were mainly distributed in the subcortical nucleus (putamen, caudate, claustrum, and right hippocampus). In addition, clusters were also seen in the left inferior/superior temporal gyrus, cerebellum, left supramarginal gyrus, and left angular gyrus. cART, combined antiretroviral therapy SIV, simian immunodeficiency virus.

inferior temporal gyrus), parietal (supramarginal gyrus, angular gyrus), occipital, insular, anterior quadrangular lobule of cerebellum positively correlated with $CD4^+$ T-cell count and $CD4^+/CD8^+$ ratio whereas the volume of the cluster in right uvula (extend to right lobule VII, gracile lobule) of cerebellum showed a negative correlation with $CD4^+$ T-cell count. GMV did not significantly correlate with viral load in CSF in both groups (Supplementary Figs. 5, http://links.lww.com/QAD/C266 and 6, http://links.lww.com/QAD/C266). All the analyses were corrected for multiple comparisons (GRF correction, voxel-level $P < 0.001$, cluster level $P < 0.05$, two-tailed).

## Discussion

In this study, we used $SIV_{mac239}$-infected Chinese origin macaques to investigate GMV, WMV, lateral ventricles,

and laboratory tests (viral load, $CD4^+$ T-cell count, and $CD4^+/CD8^+$ ratio) alterations throughout the progression of SIV infection (about 1 year). Brain volume alteration can be detected as early as 12 wpi, such differences located in total gray matter, total white matter volume, lateral ventricle volume, right caudate, left putamen, bilateral hippocampus, bilateral frontal lobe, bilateral temporal lobe, left insular, and right cerebellum. As the disease course progresses, gray matter showed generalized atrophy with lateral ventricle expansion while white matter showed a relatively mild pattern in macaques without therapy. For macaques received therapy, brain volume alteration can still be detected but to a less extent. For one macaque in the SIV+cART+ group, whole-brain GMV increased gradually with treatment, suggesting brain atrophy can be effectively relieved, even reversed, by cART. Plasma viral load was mainly linked to subcortical nucleus volume, and immunological markers were associated with widespread cortical GMV (for cART-naive macaques, thalamus volume was also associated with immunological markers).

Weight increase was not evident in SIV-infected macaques. However, macaques received cART showed a mild weight increase after a period of treatment, similar to delayed development in HIV-infected children [32]. Longitudinal changes in viral load, $CD4^+$ T-cell count, and $CD4^+/CD8^+$ ratio observed in our study aligned with that reported in SIV-infected macaque models [27,33–35]. In addition, our study indicated brain volume alterations can be detected in this model. Pathology evidence from previous research showed neuronal injury occurs 14 dpi and exacerbates with time [36]. Taken together, $SIV_{mac239}$-infected Chinese origin macaque can be a valid model to investigate HIV-induced brain morphologic alteration. But it should be noted that the most obvious brain atrophy occurred at the endpoint (about 80%). In the acute and chronic infection stage, SIV-induced GMV reduction is not obvious (in our experiment, only one macaque showed obvious whole brain atrophy whereas other macaques often showed brain atrophy less than 10%). Furthermore, brain volume fluctuated even in healthy controls, together with the usual small sample size in nonhuman primate research, caution should be taken while adopting this model in neuroscience research.

Our study showed brain atrophy can be detected as early as 12 wpi in total gray matter, total white matter volume, lateral ventricle volume, right caudate, left putamen, bilateral hippocampus, bilateral frontal lobe, bilateral temporal lobe, left insular, and right cerebellum, which may suggest these brain regions are more subtle to SIV infection. At 48 wpi, two macaques (the macaque euthanized at 47 wpi and a macaque euthanized later at 58 wpi) in SIV+cART− group showed generalized gray matter atrophy, with total WMV reduction, LV expansion. In PWH, brain atrophy has been reported in frontal lobe [37], parietal lobe [38], occipital lobe [38], temporal lobe [14,39], insula [40], cerebellar [41], subcortical nucleus (caudate, putamen, etc.) [12,41,42], and limbic system [41], suggests a generalized atrophy pattern similar to our model. In the precART era, brain atrophy was a common neuroradiologic finding in HIV-infected people, especially those in the AIDS stage [42–44], histological examination indicated neuronal loss [44,45]. In the cART era, loss of synaptic connections has been widely reported in PWH [46,47] whereas neuronal loss is barely noticed. In addition, studies from a transgenic animal model suggested dendritic degeneration precedes neuron loss [5]. Hence, the most rapid brain atrophy occurred at the endpoint (simian AIDS stage) in SIV+cART− macaques may be because of neuronal loss. One macaque in the SIV+cART+ group showed whole brain atrophy soon after infection, and at 48 wpi whole-brain GMV increased substantially, suggesting dendritic spine reduction instead of neuronal loss may contribute to the neuropathology of the detected brain atrophy with treatment just after the acute phase [27].

Viral load was positively associated with gray matter volume of multiple brain regions, especially the subcortical nucleus, within 48 weeks postinfection in both cART-naive and cART-treated macaques. As neuronal damage is thought to be mediated by the neuroinflammatory response to viral proteins and inflammatory cytokines [1], higher viral load in plasma suggests more severe inflammation in CNS, with more obvious pathological changes, such as glial cell activation and proliferation, neuron or glia edema [45], presented as increased GMV compared with SIV+cART+ group. Previous research showed SIV-infected macaques received cART have reduced CNS virus and inflammation (such as glial cell activation and proliferation, neuron or glia edema) [48]. The presented smaller volume might occur because of less severe edema or glia cell activation and proliferation. However, this conjecture would be more convincing with the corresponding pathological examination.

$CD4^+$ T-cell count has long been served as a biomarker for immune suppression, and $CD4^+/CD8^+$ ratio is associated with immune senescence, chronic inflammation, which might more accurately describe the overall immune dysfunction [49]. In our model, GMV of multiple brain regions was positively associated with immunological markers, similar to that in PWH [14,39,50]. This again, implies systematic immune status and cortical GMV are closely related. In addition, the volume of clusters in the left inferior temporal gyrus, right occipital lobe showed a negative correlation with plasma $CD4^+/CD8^+$ ratio in SIV+cART− macaques, the volume of the cluster in right uvula (extend to right lobule VIII, gracile lobule) of cerebellum showed a negative correlation with plasma CD4+ T-cell count in SIV+cART+ macaques, this may suggest that there may be a compensatory mechanism, such as increased

dendritic spine density. Nevertheless, the underlying pathological manifestations of these two clusters require further investigation.

For most of our ROIs, gray matter volume fluctuated over time, even in the healthy control group. Several reasons might contribute to this phenomenon. First, measurement error. Second, the repeated anesthesia during our experiment may influence brain volume in our macaques [51].

An important limitation of our study is the small sample size, especially for healthy controls. Further studies with larger samples are needed to test reproducibility. In addition, our study design did not include SIV-cART+ macaques, so we were unable to elucidate the effect of cART on the brain volume of healthy macaque.

In conclusion, $SIV_{mac239}$-infected Chinese origin macaque can be a valid model to investigate HIV-induced brain alteration. SIV-infection is likely to cause generalized brain atrophy, which can be effectively relieved, even reversed, by cART. The subcortical nucleus (especially caudate and putamen) was affected by viral load whereas the cortical cortex was impacted by both viral load and immunological levels (mainly). Systematic immune function is closely linked to GMV. Further studies are warranted to reveal the pathologic mechanism behind the findings.

## Acknowledgements

This research was supported by the National Natural Science Foundation of China (Grant No. 81771806, 81771909). We are grateful to the staffs of Institute of Laboratory Animal Sciences, Chinese Academy of Medical Sciences. We also thank the radiographers from Beijing Youan Hospital and Dr Xiaojie Huang for providing Dolutegravir.

### Conflicts of interest

There are no conflicts of interest.

## References

1. Saylor D, Dickens AM, Sacktor N, Haughey N, Slusher B, Pletnikov M, *et al*. **HIV-associated neurocognitive disorder - pathogenesis and prospects for treatment.** *Nat Rev Neurol* 2016; **12**:234.
2. Yarandi SS, Robinson JA, Vakili S, Donadoni M, Burdo TH, Sariyer IK. **Characterization of Nef expression in different brain regions of SIV-infected macaques.** *PLos One* 2020; **15**:e241667.
3. Hahn YK, Podhaizer EM, Farris SP, Miles MF, Hauser KF, Knapp PE. **Effects of chronic HIV-1 Tat exposure in the CNS: heightened vulnerability of males versus females to changes in cell numbers, synaptic integrity, and behavior.** *Brain Struct Funct* 2015; **220**:605–623.
4. Fitting S, Ignatowska-Jankowska BM, Bull C, Skoff RP, Lichtman AH, Wise LE, *et al*. **Synaptic dysfunction in the hippocampus accompanies learning and memory deficits in human immunodeficiency virus type-1 Tat transgenic mice.** *Biol Psychiat* 2013; **73**:443–453.
5. Michaud J, Fajardo R, Charron G, Sauvageau A, Berrada F, Ramla D, *et al*. **Neuropathology of NFHgp160 transgenic mice expressing HIV-1 Env protein in neurons.** *J Neuropath Exp Neur* 2001; **60**:574–587.
6. Kahouadji Y, Dumurgier J, Sellier P, Lapalus P, Delcey V, Bergmann JF, *et al*. **Cognitive function after several years of antiretroviral therapy with stable central nervous system penetration score.** *Hiv Med* 2013; **14**:311–315.
7. Brier MR, Wu Q, Tanenbaum AB, Westerhaus ET, Kharasch ED, Ances BM. **Effect of HAART on brain organization and function in HIV-negative subjects.** *J Neuroimmune Pharm* 2015; **10**:517–521.
8. Keifer OP Jr, Hurt RC, Gutman DA, Keilholz SD, Gourley SL, Ressler KJ. **Voxel-based morphometry predicts shifts in dendritic spine density and morphology with auditory fear conditioning.** *Nat Commun* 2015; **6**:7582.
9. Sack M, Lenz JN, Jakovcevski M, Biedermann SV, Falfán-Melgoza C, Deussing J, *et al*. **Early effects of a high-caloric diet and physical exercise on brain volumetry and behavior: a combined MRI and histology study in mice.** *Brain Imaging Behav* 2017; **11**:1385–1396.
10. Riadh N, Allagui MS, Bourogaa E, Vincent C, Croute F, Elfeki A. **Neuroprotective and neurotrophic effects of long term lithium treatment in mouse brain.** *Biometals* 2011:747–757.
11. Black JE, Isaacs KR, Anderson BJ, Alcantara AA, Greenough WT. **Learning causes synaptogenesis, whereas motor activity causes angiogenesis, in cerebellar cortex of adult rats.** *Proc Natl Acad Sci USA* 1990; **87**:5568–5572.
12. Sanford R, Fellows LK, Ances BM, Collins DL. **Association of brain structure changes and cognitive function with combination antiretroviral therapy in HIV-positive individuals.** *Jama Neurol* 2018; **75**:72.
13. Israel SM, Hassanzadeh-Behbahani S, Turkeltaub PE, Moore DJ, Ellis RJ, Jiang X. **Different roles of frontal versus striatal atrophy in HIV-associated neurocognitive disorders.** *Hum Brain Mapp* 2019; **40**:3010–3026.
14. Hassanzadeh-Behbahani S, Shattuck KF, Bronshteyn M, Dawson M, Diaz M, Kumar P, *et al*. **Low CD4 nadir linked to widespread cortical thinning in adults living with HIV.** *Neuroimage Clin* 2020; **25**:102155.
15. Haddow LJ, Godi C, Sokolska M, Cardoso MJ, Oliver R, Winston A, *et al*. **Brain perfusion, regional volumes, and cognitive function in human immunodeficiency virus–positive patients treated with protease inhibitor monotherapy.** *Clin Infect Dis* 2019; **68**:1031–1040.
16. Sarma MK, Nagarajan R, Keller MA, Kumar R, Nielsen-Saines K, Michalik DE, *et al*. **Regional brain gray and white matter changes in perinatally HIV-infected adolescents.** *NeuroImage: Clinical* 2014; **4**:29–34.
17. Castelo JMB, Courtney MG, Melrose RJ, Stern CE. **Putamen hypertrophy in nondemented patients with human immunodeficiency virus infection and cognitive compromise.** *Arch Neurol* 2007; **64**:1275.
18. Becker JT, Maruca V, Kingsley LA, Sanders JM, Alger JR, Barker PB, *et al*. **Factors affecting brain structure in men with HIV disease in the post-HAART era.** *Neuroradiology* 2012; **54**:113–121.
19. Cohen RA, Harezlak J, Schifitto G, Hana G, Clark U, Gongvatana A, *et al*. **Effects of nadir CD4 count and duration of human immunodeficiency virus infection on brain volumes in the highly active antiretroviral therapy era.** *J Neurovirol* 2010; **16**:25–32.
20. Sanford R, Ances BM, Meyerhoff DJ, Price RW, Fuchs D, Zetterberg H, *et al*. **Longitudinal trajectories of brain volume and cortical thickness in treated and untreated primary human immunodeficiency virus infection.** *Clin Infect Dis* 2018; **67**:1697–1704.
21. Correa DG, Zimmermann N, Tukamoto G, Doring T, Ventura N, Leite SC, *et al*. **Longitudinal assessment of subcortical gray matter volume, cortical thickness, and white matter integrity in HIV-positive patients.** *J Magn Reson Imaging* 2016; **44**:1262–1269.

22. Kallianpur KJ, Jahanshad N, Sailasuta N, Benjapornpong K, Chan P, Pothisri M, *et al*. **Regional brain volumetric changes despite 2 years of treatment initiated during acute HIV infection.** *AIDS* 2020; **34**:415–426.
23. Nir TM, Jahanshad N, Ching C, Cohen RA, Harezlak J, Schifitto G, *et al*. **Progressive brain atrophy in chronically infected and treated HIV+ individuals.** *J Neurovirol* 2019; **25**:342–353.
24. Perdomo-Celis F, Taborda NA, Rugeles MT. **CD8+ T-cell response to HIV infection in the era of antiretroviral therapy.** *Front Immunol* 2019; **10**:1896.
25. Fox HS, Gold LH, Henriksen SJ, Bloom FE. **Simian immunodeficiency virus: a model for neuroAIDS.** *Neurobiol Dis* 1997; **4**:265–274.
26. Fuller RA, Westmoreland SV, Ratai E, Greco JB, Kim JP, Lentz MR, *et al*. **A prospective longitudinal in vivo 1H MR spectroscopy study of the SIV/macaque model of neuroAIDS.** *BMC Neurosci* 2004; **5**:10.
27. Ling B, Veazey RS, Luckay A, Penedo C, Xu K, Lifson JD, Marx PA. **SIV(mac) pathogenesis in rhesus macaques of Chinese and Indian origin compared with primary HIV infections in humans.** *AIDS* 2002; **16**:1489–1496.
28. Xue J, Cong Z, Xiong J, Wang W, Jiang H, Chen T, *et al*. **Repressive effect of primary virus replication on superinfection correlated with gut-derived central memory CD4(+) T cells in SHIV-infected Chinese rhesus macaques.** *PLos One* 2013; **8**:e72295.
29. Gonzalez RG, Fell R, He J, Campbell J, Burdo TH, Autissier P, *et al*. **Temporal/compartmental changes in viral RNA and neuronal injury in a primate model of NeuroAIDS.** *PLos One* 2018; **13**:e196949.
30. Hikishima K, Ando K, Komaki Y, Kawai K, Yano R, Inoue T, *et al*. **Voxel-based morphometry of the marmoset brain: in vivo detection of volume loss in the substantia nigra of the MPTP-treated Parkinson' disease model.** *Neuroscience* 2015; **300**:585–592.
31. Rohlfing T, Kroenke CD, Sullivan EV, Dubach MF, Bowden DM, Grant KA, Pfefferbaum A. **The INIA19 template and NeuroMaps Atlas for primate brain image parcellation and spatial normalization.** *Front Neuroinform* 2012; **6**:27.
32. Barlow-Mosha L, Musiime V, Davies MA, Prendergast AJ, Musoke P, Siberry G, Penazzato M. **Universal antiretroviral therapy for HIV-infected children: a review of the benefits and risks to consider during implementation.** *J Int AIDS Soc* 2017; **20**:21552.
33. Liu J, Xiao Q, Zhou R, Wang Y, Xian Q, Ma T, *et al*. **Comparative analysis of immune activation markers of CD8+ T cells in lymph nodes of different origins in SIV-infected Chinese rhesus macaques.** *Front Immunol* 2016; **7**:371.
34. Smith SM, Holland B, Russo C, Dailey PJ, Marx PA, Connor RI. **Retrospective analysis of viral load and SIV antibody responses in rhesus macaques infected with pathogenic SIV: predictive value for disease progression.** *AIDS Res Hum Retroviruses* 1999; **15**:1691–1701.
35. Tavakoli-Tameh A, Janaka SK, Zarbock K, Connor O, Crosno S, Capuano KS, *et al*. **Loss of tetherin antagonism by Nef impairs SIV replication during acute infection of rhesus macaques.** *PLos Pathog* 2020; **16**:e1008487.
36. Gonzalez RG, Cheng LL, Westmoreland SV, Sakaie KE, Becerra LR, Lee PL, *et al*. **Early brain injury in the SIV-macaque model of AIDS.** *AIDS* 2000; **14**:2841–2849.
37. Rubin LH, Meyer VJ, J. Conant R, Sundermann EE, Wu M, Weber KM, *et al*. **Prefrontal cortical volume loss is associated with stress-related deficits in verbal learning and memory in HIV-infected women.** *Neurobiol Dis* 2016; **92**:166–174.
38. Li J, Gao L, Wen Z, Zhang J, Wang P, Tu N, *et al*. **Structural covariance of gray matter volume in HIV vertically infected adolescents.** *Sci Rep-Uk* 2018; **8**:1182.
39. Küper M, Rabe K, Esser S, Gizewski ER, Husstedt IW, Maschke M, Obermann M. **Structural gray and white matter changes in patients with HIV.** *J Neurol* 2011; **258**:1066–1075.
40. Zhou Y, Li R, Wang X, Miao H, Wei Y, Ali R, *et al*. **Motor-related brain abnormalities in HIV-infected patients: a multimodal MRI study.** *Neuroradiology* 2017; **59**:1133–1142.
41. Kallianpur KJ, Shikuma C, Kirk GR, Shiramizu B, Valcour V, Chow D, *et al*. **Peripheral blood HIV DNA is associated with atrophy of cerebellar and subcortical gray matter.** *Neurology* 2013; **80**:1792–1799.
42. Aylward EH, Henderer JD, McArthur JC, Brettschneider PD, Harris GJ, Barta PE, Pearlson GD. **Reduced basal ganglia volume in HIV-1-associated dementia: results from quantitative neuroimaging.** *Neurology* 1993; **43**:2099–2104.
43. Navia BA, Cho ES, Petito CK, Price RW. **The AIDS dementia complex: II. Neuropathology.** *Ann Neurol* 1986; **19**:525–535.
44. Everall IP, Luthert PJ, Lantos PL. **Neuronal loss in the frontal cortex in HIV infection.** *Lancet* 1991; **337**:1119–1121.
45. Everall IP, Luthert PJ, Lantos PL. **Neuronal number and volume alterations in the neocortex of HIV infected individuals.** *J Neurol Neurosurg Psychiatry* 1993; **56**:481–486.
46. Green MV, Raybuck JD, Zhang X, Wu MM, Thayer SA. **Scaling synapses in the presence of HIV.** *Neurochem Res* 2019; **44**:234–246.
47. Ellis R, Langford D, Masliah E. **HIV and antiretroviral therapy in the brain: neuronal injury and repair.** *Nat Rev Neurosci* 2007; **8**:33–44.
48. Zink MC, Brice AK, Kelly KM, Queen SE, Gama L, Li M, *et al*. **Simian immunodeficiency virus–infected macaques treated with highly active antiretroviral therapy have reduced central nervous system viral replication and inflammation but persistence of viral DNA.** *J Infect Dis* 2010; **202**:161–170.
49. McBride JA, Striker R. **Imbalance in the game of T cells: what can the CD4/CD8 T-cell ratio tell us about HIV and health?** *PLos Pathog* 2017; **13**:e1006624.
50. Wright PW, Pyakurel A, Vaida FF, Price RW, Lee E, Peterson J, *et al*. **Putamen volume and its clinical and neurological correlates in primary HIV infection.** *AIDS* 2016; **30**:1789–1794.
51. Zhao T, Chen Y, Sun Z, Shi Z, Qin J, Lu J, *et al*. **Prenatal sevoflurane exposure causes neuronal excitatory/inhibitory imbalance in the prefrontal cortex and neurofunctional abnormality in rats.** *Neurobiol Dis* 2020; **146**:105121.